



OPEN ACCESS

EDITED BY

Antonio Osuna,
University of Granada, Spain

REVIEWED BY

Jose Piñero,
University of La Laguna, Spain
Mercedes Gomez,
University of Granada, Spain

*CORRESPONDENCE

Gabriel Espinosa

✉ gabriel.rodolfo.espinosa.espinosa@vetmed.uni-giessen.de

†These authors have contributed equally to this work and share first authorship

RECEIVED 21 June 2023

ACCEPTED 28 August 2023

PUBLISHED 03 October 2023

CITATION

Espinosa G, Conejeros I, Rojas-Barón L, Hermosilla CR and Taubert A (2023) *Besnoitia besnoiti*-induced neutrophil clustering and neutrophil extracellular trap formation depend on P2X1 purinergic receptor signaling. *Front. Immunol.* 14:1244068. doi: 10.3389/fimmu.2023.1244068

COPYRIGHT

© 2023 Espinosa, Conejeros, Rojas-Barón, Hermosilla and Taubert. This is an open-access article distributed under the terms of the [Creative Commons Attribution License \(CC BY\)](https://creativecommons.org/licenses/by/4.0/). The use, distribution or reproduction in other forums is permitted, provided the original author(s) and the copyright owner(s) are credited and that the original publication in this journal is cited, in accordance with accepted academic practice. No use, distribution or reproduction is permitted which does not comply with these terms.

Besnoitia besnoiti-induced neutrophil clustering and neutrophil extracellular trap formation depend on P2X1 purinergic receptor signaling

Gabriel Espinosa^{*†}, Iván Conejeros[†], Lisbeth Rojas-Barón, Carlos Rodrigo Hermosilla and Anja Taubert

Institute of Parasitology, Justus Liebig University Giessen, Giessen, Germany

Bovine besnoitiosis is a re-emerging cattle disease caused by the cyst-forming apicomplexan parasite *Besnoitia besnoiti*. Neutrophil extracellular trap (NET) formation represents an efficient innate immune mechanism of polymorphonuclear neutrophils (PMN) against apicomplexan parasites, including *B. besnoiti*. PMN purinergic signaling was proposed as a critical factor for NET formation. One important purinergic ligand is ATP, which is recognized as a danger signal and released into the extracellular space acting as an autocrine/paracrine signaling molecule. ATP-driven effects on PMN via the nucleotide P2 receptor family include chemotaxis, reactive oxygen species (ROS) production, and NET formation. So far, data on both PMN ATP concentrations and the role of ATP as a key modulator of purinergic signaling in *B. besnoiti* tachyzoite-triggered bovine NETosis is scarce. Current data showed that *B. besnoiti* tachyzoite exposure to bovine PMN neither changed total PMN ATP nor extracellular ATP quantities even though it significantly triggered NET formation. Moreover, *B. besnoiti* tachyzoite-exposed PMN revealed enhanced oxygen consumption rates (OCR) as quantified by the Seahorse metabolic analyzer. Exogenous supplementation of ATP or non-hydrolyzable ATP (ATP γ S) led to increased extracellular acidification rates (ECAR) but failed to alter tachyzoite-induced oxidative responses (OCR) in exposed PMN. In addition, exogenous supplementation of ATP γ S, but not of ATP, boosted *B. besnoiti* tachyzoite-induced anchored NET formation. Referring to purinergic signaling, *B. besnoiti* tachyzoite-triggered anchored NET formation revealed P2X1 purinergic as receptor-dependent since it was blocked by the P2X1 inhibitor NF449 at an IC₅₀ of 1.27 μ M. In contrast, antagonists of P2Y2, P2Y6, P2X4, and P2X7 purinergic receptors all failed to affect parasite-driven NETosis. As an interesting finding, we additionally observed that *B. besnoiti* tachyzoite exposure induced PMN clustering in a P2X1-dependent manner. Thus, we identified P2X1 purinergic receptor as a pivotal molecule for both *B. besnoiti* tachyzoite-induced PMN clustering and anchored NET formation.

KEYWORDS

PMN, *Besnoitia besnoiti*, NET formation, ATP, purinergic receptors, immunometabolism

1 Introduction

Besnoitia besnoiti is a cyst-forming apicomplexan parasite closely related to *Toxoplasma gondii* and *Neospora caninum*. It is the causal agent of bovine besnoitiosis, a severe but mainly non-fatal disease with significant economic impact in many countries in Africa, Asia, and Europe (1, 2). In 2010, the disease was classified as an emerging disease by the European Food Safety Authority (EFSA). Typical clinical signs of acute besnoitiosis are pyrexia, photophobia, lacrimation, tachypnoe, acute orchitis, and subcutaneous edema. In chronically infected cattle, parasitic cysts develop in various organs, including skin, vascular walls, sclera, and other non-intestinal mucous membranes. Typically, skleroderma with skin thickening, abrasion, and alopecia occurs. Moreover, skin alterations of the udder impair proper milking. Chronic *B. besnoiti* infections of bulls may cause orchitis leading to transient or permanent infertility (3). *B. besnoiti* can be mechanically transmitted by hematophagous tabanids (*Tabanus* spp.) and biting muscids like *Stomoxys calcitrans*; the role of transmission via mating remains unclear so far. To date, the definitive host of *B. besnoiti* is unknown (3, 4).

Referring to immunological responses in *B. besnoiti* tachyzoite-infected cattle, (immune) histochemical studies show leukocyte infiltration in the dermis of affected animals (5), indicating that early host defense responses are important for disease progression. Polymorphonuclear neutrophils (PMN) represent the most abundant leukocyte population in the blood and are amongst the first innate immune cell types responding against infection. PMN also participate in the resolution of inflammation and wound healing (6). In general, PMN react against a variety of invasive pathogens, such as bacteria, viruses, fungi, protozoan, and metazoan parasites. Different PMN-derived effector mechanisms have been demonstrated, including the release of immunomodulatory molecules [e.g., cytokines and chemokines], phagocytosis, production of reactive oxygen species (ROS), and release of neutrophil extracellular traps (NETs) (6–9). Referring to the latter mechanism, NETs are typically composed of DNA, histones, and microbicidal peptides and bear the capacity to kill certain pathogens like bacteria (10) or to limit pathogen spread in infected organisms by local trapping activities (11). NETs are released via a cell death process known as NETosis (12). NETosis is either linked to a nicotinamide adenine dinucleotide phosphate (NADPH) oxidase (NOX)-dependent or NOX-independent cellular mechanism, which triggers nuclear chromatin decondensation facilitated by protein arginine deiminase 4 (PAD4)-mediated citrullination of histones, fast actin cytoskeleton disassembly, microtubules remodeling, and shedding of plasma membrane microvesicles containing granules and cytosolic components. Following this, enzymes like neutrophil elastase (NE) and myeloperoxidase (MPO) translocate to the nucleus and fuse with chromatin. Finally, PMN membrane disintegration is either mediated by enhanced ROS production or by lytic proteins like gasdermin D mediating membrane pore formation and subsequent NET extrusion into the extracellular matrix (11–17).

The protozoan parasite-driven NET release is reported for *Eimeria bovis* (18, 19), *Eimeria arloingi* (20), *Toxoplasma gondii* (21–23), *Cryptosporidium parvum* (24), *Neospora caninum* (25–27),

Trypanosoma brucei brucei (28), and *B. besnoiti* (29–32). Notably, *B. besnoiti* tachyzoite-driven NETosis seemed stage-independent since bradyzoites were also proven to trigger NETosis in bovine PMN (33). Referring to signaling cascades upstream of *B. besnoiti* tachyzoite-driven NET formation, tachyzoite exposure to PMN induced the phosphorylation of AMP-activated kinase α (AMPK α), and a positive correlation between LC3B-positive PMN and NET formation is described (31). More recently, metabolic responses of *B. besnoiti* tachyzoite-exposed bovine PMN revealed enhanced catabolism of glucose and serine, accompanied by increased glutamate production (32). Secondary metabolites in *B. besnoiti* tachyzoite-exposed PMN appeared pivotal for NET formation since chemical inhibition of lactate release, pyruvate dehydrogenase, α -ketoglutarate dehydrogenase, and transketolase significantly affected cell-free NET formation, thereby indicating a key role of pyruvate- and lactate-mediated metabolic pathways. Interestingly, tachyzoite-induced NET formation was also significantly blocked by treatments with oligomycin A (inhibitor of ATP synthase) and NF449 (purinergic receptor P2X1 antagonist), suggesting a key role of ATP-related responses in tachyzoite-driven NETosis (32).

Intracellular ATP represents the main source of energy driving almost all cell functions. However, ATP also plays a key role in purinergic signaling. Hence, stressed cells release ATP as a danger and “find me” signal, thereby guiding the migration of purinergic receptor-expressing leukocytes (e.g., PMN) which then respond to extracellular ATP and related nucleotides. In general, three major families of purinergic receptors are described based on their pharmacological and structural properties. P2X receptors function as ATP-gated ion channels that facilitate the influx of extracellular cations, including calcium. In contrast, P2Y receptors represent G protein-coupled receptors (GPCRs), which recognize ATP and several other nucleotides including ADP, UTP, UDP, and UDP-glucose. Moreover, P1 receptors are also GPCRs that recognize adenosine (34–37). Purinergic signaling in PMN regulates critical PMN functions via paracrine and autocrine (feedback) mechanisms. For example, the release of ATP via pannexin-1 (PANX1) channels to the extracellular environment regulates PMN chemotaxis, rolling/adhesion/transmigration, ROS generation, NETosis, and apoptosis (36, 38–43).

The aim of the current work was to analyze the role of purinergic signaling and the metabolic state of PMN in *B. besnoiti* tachyzoite-induced NET formation. Early PMN activation was studied via oxygen consumption (OCR) and extracellular acidification rates (ECAR) using the Seahorse technology. Moreover, the role of selected molecules of the purinergic signaling cascade in relevant PMN functions like clustering and NET formation was studied.

2 Materials and methods

2.1 Ethics statement

This study was performed in accordance with the Justus Liebig University Giessen Animal Care Committee Guidelines. Protocols

were approved by the Ethics Commission for Experimental Animal Studies of the Federal State of Hesse (Regierungspräsidium Giessen; GI 18/10 Nr. V 2/2022; JLU-No. 0002_V) and are in accordance with European Animal Welfare Legislation: ART13TFEU and currently applicable German Animal Protection Laws.

2.2 Host cell culture and *B. besnoiti* tachyzoite maintenance

All experiments of the current study were performed with tachyzoite stages of the apicomplexan parasite *B. besnoiti* (strain Bb-Evora04). Madin-Darby bovine kidney (MDBK) cells were used as host cells for *B. besnoiti* tachyzoite in *in vitro* production. MDBK cell layers were cultured in 75 cm² plastic tissue culture flasks (Greiner) at 37°C/5% CO₂ atmosphere using RPMI 1640 (Sigma-Aldrich) cell culture medium supplemented with 5% fetal bovine serum (FBS, 10270-106, Gibco) and 1% penicillin/streptomycin (both 500 mg/ml, P4333, Sigma-Aldrich). MDBK cell layers were infected at 80% confluency with 2.4×10⁷ *B. besnoiti* tachyzoites. Tachyzoites released from host cells were collected from the supernatants, filtered through a 5 µm syringe filter (Merck Millipore), washed, and pelleted (400×g, 12 min) prior to re-suspension in RPMI 1640 cell culture medium (supplemented with 5% FBS and 1% penicillin/streptomycin). Tachyzoite numbers were determined in a Neubauer chamber, and parasite stages were placed at 37°C/5% CO₂ atmosphere for further experimental use.

2.3 Bovine PMN isolation

Healthy adult dairy cows served as blood donors. Animals were bled by puncturing the jugular vein, and peripheral blood was collected in heparinized sterile plastic tubes (Kabe Labortechnik). A measurement of 20 mL of heparinized blood was re-suspended in 20 mL sterile PBS with 0.02% EDTA (CarlRoth), carefully layered on top of 12 ml Histopaque-1077 separating solution (density = 1.077 g/L; 10771, Sigma-Aldrich) and centrifuged (800×g, 45 min) without brake. After removal of plasma and peripheral blood mononuclear cells, the cell pellet was suspended in 20 mL of lysis buffer (5.5 mM NaH₂PO₄, 10.8 mM KH₂PO₄, and pH 7.2) and gently mixed for 60 s to lyse erythrocytes. Osmolarity was rapidly restored by the addition of 10 mL hypertonic buffer (462 mM NaCl, 5.5 mM NaH₂PO₄, 10.8 mM KH₂PO₄, and pH 7.2) and 10 mL of Hank's balanced salt solution (14065-049, Gibco). The lysis step was repeated twice until no erythrocytes were visible. PMN were then suspended in 5 mL of HBSS, counted in a Neubauer chamber, and allowed to rest on ice for 30 min prior to any experimental use.

2.4 Scanning electron microscopy

Bovine PMN were co-cultured at 37°C and 5% CO₂ with *B. besnoiti* tachyzoites at a 1:4 ratio for 60 min on 10 mm coverslips

(Thermo Fisher Scientific) pre-coated with 0.01% poly-L-lysine (Sigma-Aldrich). After incubation, cells were fixed in 2.5% glutaraldehyde (Merck), post-fixed in 1% osmium tetroxide (Merck), washed in distilled water, dehydrated, critical point dried by CO₂ treatment, and sputtered with gold. Finally, all samples were analyzed via a Philips XL30 scanning electron microscope at the Institute of Anatomy and Cell Biology, Justus Liebig University Giessen, Germany.

2.5 Immunofluorescence microscopy

Bovine PMN were co-cultured with *B. besnoiti* tachyzoites at a 1:6 ratio for 4 h (37°C, 5% CO₂ atmosphere) on fibronectin- (2.5 µg/mL) pretreated coverslips (15 mm diameter, Thermo Fisher Scientific), fixed in 4% paraformaldehyde (Merck), and stored at 4°C until further use. For NET visualization, DAPI (Fluoromount G, ThermoFisher, 495952) was used to stain DNA. Anti-histone (clone TNT-1, 1:1000; Merck Millipore #MAB3864, Darmstadt, Germany) and anti-NE (AB68672, 1:1000, Abcam, Cambridge, UK) antibodies were used to detect respective proteins on NET structures. In addition, an in-house hyperimmune serum against *B. besnoiti* was used (1:100) to stain tachyzoite stages. For antibody-related reactions, fixed samples were washed three times with PBS, blocked with 1% bovine serum albumin (BSA, Sigma-Aldrich, Steinheim, Germany, 30 min, RT), and incubated in corresponding primary antibody solutions (1 h, RT). After three washings in PBS, samples were incubated in secondary antibody solutions (Alexa Fluor 488 goat anti-mouse IgG or Alexa Fluor 405 goat anti-rabbit IgG, both Life Technologies, Eugene, USA, 60 min, 1:1000, RT). Finally, samples were washed three times in PBS and mounted in an anti-fading buffer (Fluoromount G, ThermoFisher, 495952). Image acquisition was performed in a Ti2-A inverted microscope (Nikon) equipped with a white LED epifluorescence lamp using the NIS-Elements v 5.11 software (Nikon) and applying identical brightness and contrast conditions within the datasets of each biological experiment.

2.6 Quantification of “cell-free” and “anchored” NETs

Bovine PMN suspended in RPMI 1640 medium were confronted with *B. besnoiti* tachyzoites (4 h, 37°C, 5% CO₂) at a PMN/tachyzoite ratio of 1:6 (2×10⁵ PMN:1.2×10⁶ tachyzoites, 96-well format) in the presence of non-modified ATP (P1132, Promega, USA), non-hydrolyzable ATP (ATPγS; 0.05-50 µM; 4080, Tocris, UK), or purinergic receptor antagonists (see Table 1) at a concentration range of 0.1-100 µM. After incubation, sample supernatants were analyzed for “cell-free” NETs. The remaining cells at the well bottoms were estimated for “anchored” NETs according to (44). Therefore, picogreen (Invitrogen, Eugene, USA, 1:200 dilution in 10 mM Tris base buffered with 1 mM EDTA, 50 µl/well) was added to each supernatant or pellet sample. Extracellular DNA was quantified

TABLE 1 Purinergic receptor antagonists.

Receptor	Antagonist	Cat. number (Company)
P2Y1	MRS 2179	0900 (Tocris)
P2Y6	MRS 2578	2146 (Tocris)
P2X1	NF449	1391 (Tocris)
P2X4	5-BDBD	3579 (Tocris)
P2X7	AZ10606120	3323 (Tocris)

by picogreen-derived fluorescence intensities using an automated microplate reader (Varioskan, Thermo Scientific) at 484 nm excitation/520 nm emission as described elsewhere (26, 30).

2.7 Measurement of total and extracellular ATP concentrations

Bovine PMN of 1×10^6 from three blood donors were confronted with *B. besnoiti* tachyzoites (1:6 ratio) in HBSS $1 \times (14065-049, Gibco)$ and incubated at $37^\circ\text{C}/5\% \text{CO}_2$ for both 15 s and 15 min. For positive controls, cells were stimulated with PMA/ionomycin ($100 \text{ nM}/5 \mu\text{M}$) and HBSS supplemented with 1 M NaCl. After incubation on ice for 5 min, cells were pelleted ($600 \times g, 5 \text{ min}$) and supernatants were recovered for extracellular ATP quantification using an ATP Determination kit (A22066; Invitrogen) according to the manufacturer's instructions. For the estimation of PMN total ATP concentration, whole cell pellets were analyzed by the CellTiter-Glo luminescent Cell viability assay (G7571, Promega) following the manufacturer's instructions. All samples were analyzed by luminometry using an automated reader (Luminoskan Flash).

2.8 Quantification of PMN oxygen consumption rates and extracellular acidification rates

Activation of bovine PMN was monitored using the Seahorse XF analyzer (Agilent). Briefly, 1×10^6 PMN from three blood donors were pelleted [$500 \times g, 10 \text{ min}$, room temperature (RT)]. The cell pellets were re-suspended in 0.25 ml of XF assay medium (Agilent) supplemented with 2 mM of L-glutamine, 1 mM pyruvate, and 10 mM glucose. A total of 2×10^5 cells were gently placed in each well of an eight-well XF analyzer plate (Agilent) pre-coated for 30 min with 0.001% poly-L-lysine (Sigma-Aldrich). Then, the XF assay medium (Agilent) was adjusted to 180 μl total volume per well and cells were incubated at 37°C without CO_2 supplementation for 45 min before Seahorse measurements. ATP, ATP γS (0.05–50 μM), and *B. besnoiti* (1.2×10^6 tachyzoites) were suspended in an XF assay medium and supplemented to the cells via instrument-own injection ports after baseline measurements. The total assay duration was 240 min. Background subtraction and determination of OCR/ECAR registries were performed by using the Seahorse Agilent analytics platform (<https://seahorseanalytics.agilent.com>).

2.9 Assessment of NF449-mediated effects on PMN viability by flow cytometry

In order to determine potential NF449-driven effects on PMN apoptosis and necrosis rates, PMN suspensions ($2 \times 10^5/200 \mu\text{l}$ HBSS) were placed into 5 mL polystyrene round-bottom tubes (352052, Falcon, Corning USA) and treated with NF449 (10–100 μM) for 4 h at $37^\circ\text{C}/5\% \text{CO}_2$. PMN were then pelleted ($600 \times g, 8 \text{ min}$) and stained using the Annexin V-FITC/PI double staining apoptosis detection kit (ab14085, Abcam) following the manufacturer's instructions and analyzed with a BD Accuri C6 Plus Flow Cytometer (BD, USA). FlowJo v10.8.1 software was used to determine the apoptosis/necrosis rate.

2.10 Statistical analysis

All experiments were repeated at least three times. Statistical significance was defined by a p -value < 0.05 . The p -values were determined by applying the following analyses: unpaired two-way t-tests were used for Seahorse-based metabolic measurements. Unpaired two-way t-tests and one-way ANOVA followed by Tukey's multiple comparisons test were applied to ATP quantification experiments. One-way ANOVA followed by a Dunnett's multiple comparison test was used to analyze extracellular DNA quantification experiments. Kruskal Wallis's followed by Dunn's multiple comparisons test was applied to extracellular DNA quantification assays using purinergic receptors inhibitors. One-way ANOVA followed by Tukey's multiple comparisons test was used to analyze clustering experiments. Bar graphs represent the mean \pm SD, and statistical analysis was generated using Graph Pad software (v. 7.03).

3 Results

3.1 *B. besnoiti* tachyzoite-exposed bovine PMN release NETs entrapping tachyzoites

To confirm the functional capacity of *B. besnoiti* tachyzoites to induce NETosis in bovine PMN, we analyzed parasite-confronted PMN for NET formation by SEM and immunofluorescence analysis. SEM showed that *B. besnoiti* tachyzoite-exposed PMN indeed released NETs in comparison to unstimulated PMN (Figures 1A, B) with several tachyzoites being firmly entrapped by these structures (Figures 1C, D; arrows). Of note, the aberrant morphology of entrapped tachyzoites in Figure 1D strongly suggested that these stages were dead. To confirm NET identity, classical proteins of NETs were visualized by immunostaining. Here, co-localization of extracellular DNA with histone (i.e., H1) and neutrophil elastase were verified for *B. besnoiti* tachyzoite-driven NETs. Some of these NET fibers were in direct contact with *B. besnoiti* tachyzoites, entrapping the parasites (Figures 1E, F).

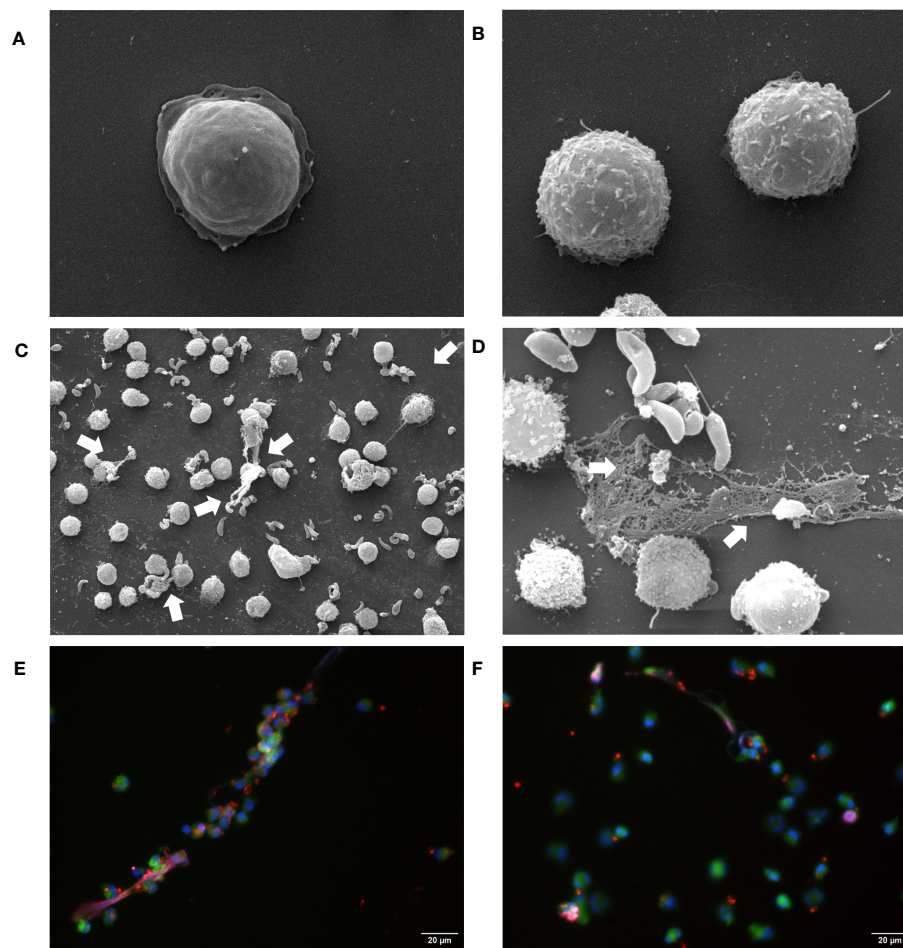


FIGURE 1

B. besnoiti tachyzoites are trapped in released NETs. (A, B) Unstimulated PMN. NETs defined as extracellular chromatin filaments containing proteins like neutrophil elastase and histone H1 formed a network in contact with *B. besnoiti* tachyzoites, as visualized via SEM (C, D) and immunostaining (E, F). White arrows indicate entrapped *B. besnoiti* tachyzoites. Co-localization of DNA (DAPI, blue); *B. besnoiti* tachyzoites (red); Histone H1 clone TNT-1 staining (pink) and neutrophil elastase (NE, green).

3.2 Exposure to *B. besnoiti* tachyzoites induces oxidative responses in bovine PMN

To explore parasite-driven changes in the energetic status and oxidative responses of *B. besnoiti* tachyzoite-confronted PMN, we analyzed PMN metabolic parameters by means of oxygen consumption rates (OCR) and extracellular acidification rates (ECAR) (Figure 2). *B. besnoiti* tachyzoite supplementation to PMN induced a significant increase in OCR ($p < 0.01$), whilst ECAR was not affected (Figures 2A, B). Given that ATP is involved in PMN metabolic and signaling responses, the effect of non-modified ATP supplementation at increasing concentrations was evaluated. Overall, ATP supplementation failed to change oxidative responses (OCR) (Figure 2C) but led to a significant ($p < 0.05$) increase in ECAR at a concentration of 50 μM (Figure 2D). Based on these data, the influence of ATP on *B. besnoiti* tachyzoite-induced activation of PMN was evaluated on the level of additive effects. Therefore, PMN

were pre-treated with ATP (50 μM) and then exposed to *B. besnoiti* tachyzoites (PMN: tachyzoites, 1:6). However, ATP pretreatments neither changed the parasite-driven increase in OCR nor ECAR levels (Figures 3A, B). A rapid increase in ECAR after ATP supplementation (Figure 3B, unfilled circles) was observed when compared to plain XF RPMI medium (Figure 3B; filled black circles, $p < 0.05$). Energetic mapping (Figure 3C) indicated that *B. besnoiti* tachyzoite exposure induced a shift toward aerobic metabolism in PMN (Figure 3C), whilst ATP supplementation rather shifted PMN into a glycolytic status (Figure 3C). When the non-hydrolyzable variant of ATP (ATPγS; Figures 3D, E) was used, a modest but significant increase in PMN OCR and ECAR was observed, indicating that PMN are activated and move into an energetic status. Again, the addition of ATPγS did not alter the response to *B. besnoiti* tachyzoites (Figures 3D, E). Overall, the tachyzoite-induced OCR increase was neither changed by ATP nor by ATPγS supplementation, thereby suggesting a pivotal role of oxygen consumption in parasite-driven activation of bovine PMN.

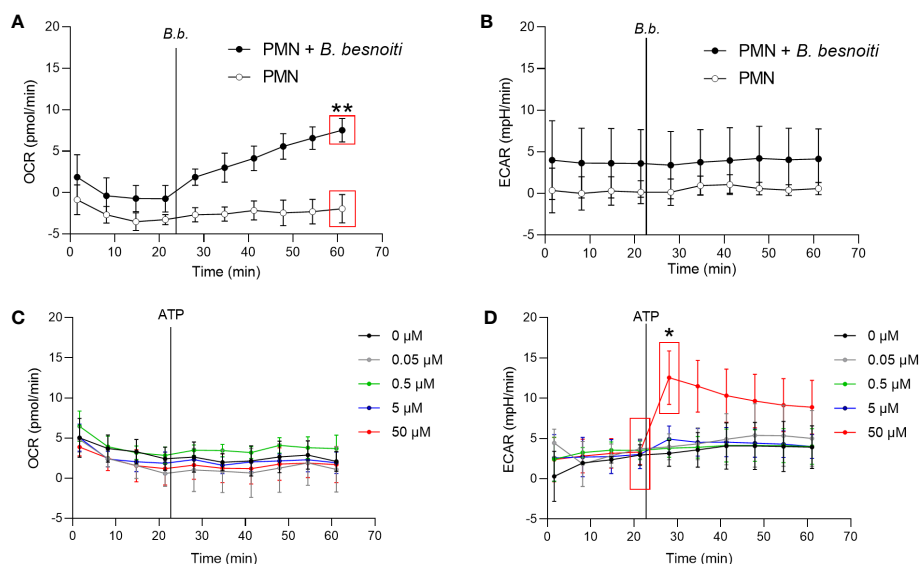


FIGURE 2

Exposure to *B. besnoiti* tachyzoites induces oxygen consumption in bovine PMN. In the absence of CO₂, 2x10⁵ PMN were incubated in XF RPMI media for 45 min. Four basal measurements were made and then either *B. besnoiti* tachyzoites (A, B) or ATP (0.05–50 μM; (C, D)) was supplemented at the time point indicated by a vertical line. OCR (A, C) and ECAR (B, D) values were obtained by Seahorse technology and plotted over time ($n = 3$, for each condition). All data are shown as mean \pm SD; p -values were calculated by unpaired two-tailed t -test analysis ($n = 3$).

3.3 *B. besnoiti* tachyzoite exposure does not affect total ATP concentration in bovine PMN

To investigate a potential change in extracellular ATP and total PMN ATP levels in tachyzoite-PMN co-cultures, ATP concentrations were analyzed at 15 s or 15 min of confrontation by luminometry (Figure 4). For positive controls, stimulation of PMN with hypersaline buffer and PMA/ionomycin were used. Exogenous ATP levels were measured in supernatants of PMN treated with a hypertonic buffer for 15 s and indeed showed a significant increase ($p < 0.001$) in extracellular ATP (Figure 4A). Furthermore, total ATP levels of bovine PMN were estimated in PMN stimulated with PMA and ionomycin for 15 and 60 min and revealed a continuous drop in ATP levels signifying ATP consumption over time ($p < 0.0001$) (Figure 4B). However, when PMN were exposed to *B. besnoiti* tachyzoites, neither changes in extracellular ATP concentration nor total PMN ATP concentration were detected (Figures 4C–E).

3.4 Non-hydrolyzable ATP boosts *B. besnoiti* tachyzoite-induced anchored NET formation

Given that a high extracellular ATP represents a danger signal and may influence general PMN effector mechanisms, we studied the effects of exogenous ATP on parasite-driven NETosis. NET quantification based on picogreen-derived fluorescence intensities was performed allowing for “cell-free” and “anchored” NET differentiation, thereby reflecting the late

phase of NETosis. Therefore, PMN were pre-stimulated with non-modified ATP or ATP γ S in a dose-dependent manner and then confronted with *B. besnoiti* tachyzoites (Figure 5). As expected, parasite-exposed PMN showed a significant increase in anchored NETs ($p < 0.05$) compared to medium-stimulated controls (Figure 5D). Dose-dependent treatments with exogenous non-modified ATP treatment neither affected basal nor tachyzoite-induced NET formation (Figures 5A–D). In contrast, ATP γ S treatments resulted in a significant increase in basal-anchored ($p < 0.0001$) and cell-free ($p < 0.01$) NET formation in plain PMN at 50 μM concentration (Figures 5E, G). Interestingly, in the case of *B. besnoiti* tachyzoite-exposed PMN, ATP γ S treatments exclusively induced an increase in the release of anchored NETs but not of cell-free NETs ($p < 0.01$; Figure 5H).

3.5 P2X1 inhibition by NF449 antagonist blocks *B. besnoiti* tachyzoite-induced anchored NET formation

Given that exogenous ATP seemed to play a role in NET induction, we further investigated the relevance of purinergic signaling pathways in *B. besnoiti* tachyzoite-induced NETosis. To monitor the role of different purinergic receptors, PMN were pre-treated with receptor antagonists of different P2X (P2X1, P2X4, and P2X7) and P2Y (P2Y1 and P2Y6) receptors at different concentrations (see Table 1) and then confronted with parasite stages (Figure 6). In antagonist-free controls, PMN confrontation with *B. besnoiti* tachyzoites resulted in a significant increase ($p < 0.05$) in anchored NET formation when compared to controls. In

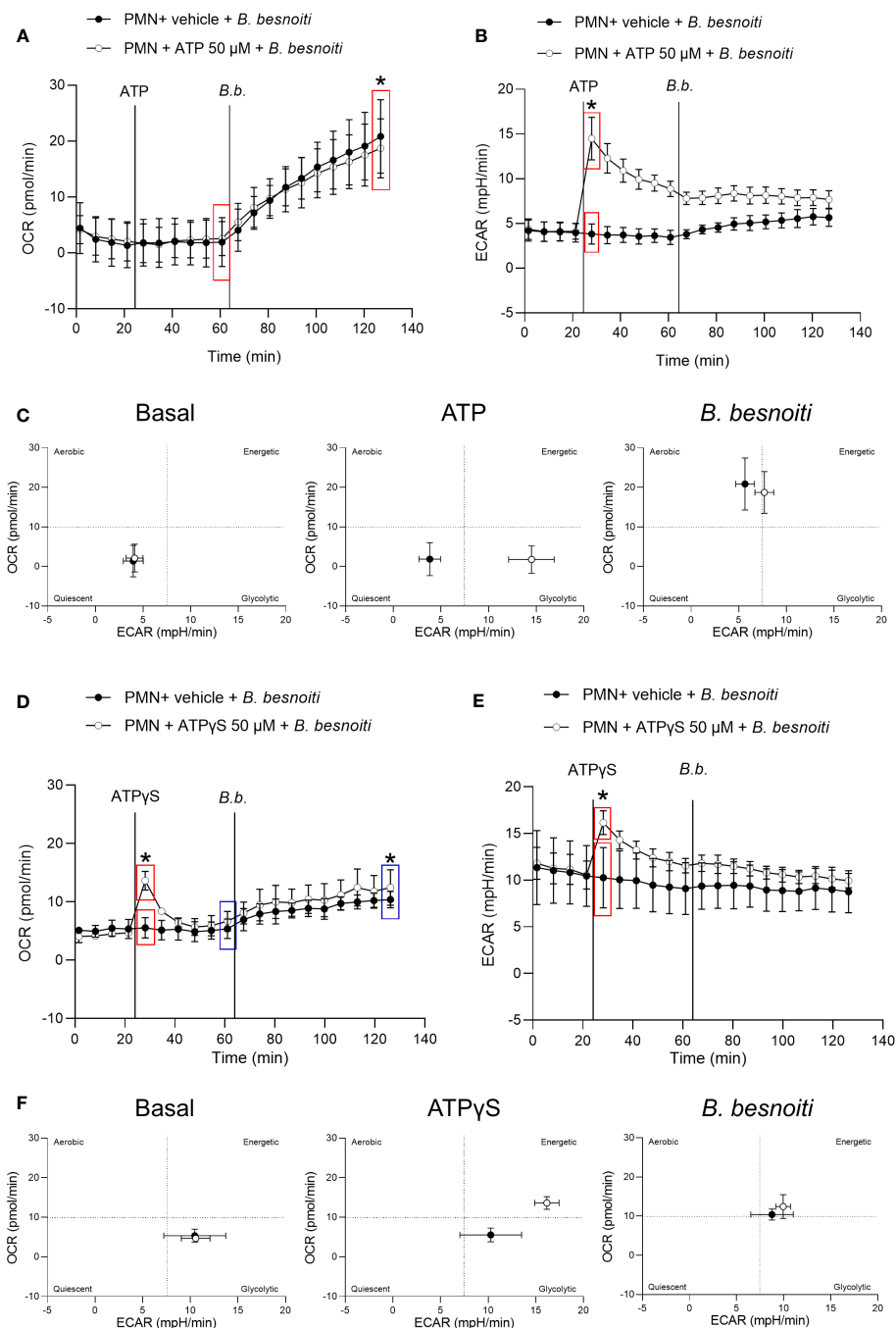


FIGURE 3

Exposure to *B. besnoiti* tachyzoites induces a metabolic shift toward aerobic carbohydrate catabolism in bovine PMN. After basal measurements, PMN were treated with ATP, ATPγS (50 μM), or vehicle, followed by supplementation of *B. besnoiti* tachyzoites as indicated by vertical lines. Differences in OCR and ECAR from means in the same curve and sharing boxes of the same color were calculated (A, B, D, E). Energetic maps (C, F) were generated by presenting OCR (Y-axis) and ECAR (X-axis) as means of the different measurements over time. All data are shown as mean ± SD; *p*-values were calculated by unpaired *t*-test (A, B, *n* = 6; D, E *n* = 3).

line with previous data (32), NF449 pre-treatments targeting the purinergic P2X1 receptor resulted in a significant decrease in *B. besnoiti* tachyzoite-triggered anchored NETs ($p < 0.05$) when compared to non-treated PMN (Figure 6J). However, all other treatments (pharmacological inhibition of P2X4, P2X7, P2Y1, and P2Y6 receptors) failed to affect parasite-triggered anchored or cell-free NET formation (Figures 6A–H). Besides antagonist pre-

treatments, the inhibitors were also added 40 min after *B. besnoiti* tachyzoite exposure to determine if any of the antagonists were capable of reverting parasite-induced NET formation, previously described as a “point of no return” and defined as consumption of intracellular ATP by PMN after 30–40 min of activation (16). In this experimental setting, a selective efficacy of NF449 was confirmed since exclusively this treatment significantly decreased *B. besnoiti*

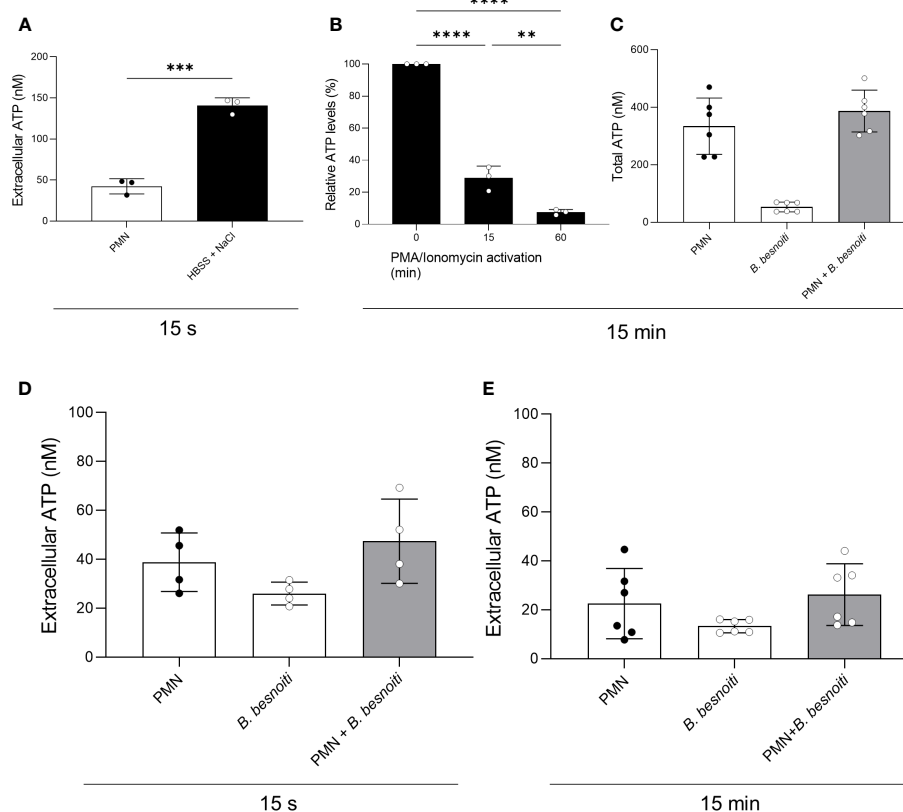


FIGURE 4

Total PMN ATP and extracellular ATP concentration in *B. besnoiti* tachyzoite-PMN co-cultures. (A) For positive control of ATP release, PMN were treated for 15 s with a hypertonic buffer (HBSS supplemented with 1 M sodium chloride). $***p < 0,001$. (B) For positive control for PMN ATP consumption, PMN were stimulated with PMA/ionomycin (100 nM/5 μ M) for 15 and 60 min. $**p < 0,01$; $****p < 0,0001$. (C–E) To assess parasite-driven effects on PMN ATP release and consumption, bovine PMN were confronted with *B. besnoiti* tachyzoites (1:6) for 15 s and 15 min. ATP in PMN (total ATP) or supernatants (extracellular ATP) was measured with a commercial kit. All data are shown as mean \pm SD; p -values were calculated by unpaired two-way t-test (A), or one-way ANOVA followed by Tukey's multiple comparison (B–E) analysis (A, B, $n = 3$; D, $n = 4$; C, $n = 6$).

tachyzoite-triggered anchored ($p < 0.01$) and cell-free ($p < 0.05$) NETs (Figures 7C, D). The sum of these data indicated that tachyzoite-induced NETosis selectively depends on P2X1-mediated signaling.

3.6 NF449 blocks *B. besnoiti* tachyzoite-induced NET formation in a dose-dependent manner and without affecting cell viability

Since NF449 was the only inhibitor that consistently reduced *B. besnoiti* tachyzoite-induced NET formation, we further studied the dose dependency of these reactions and eventual ATP-driven changes but also controlled the potential effects of this P2X1 antagonist on PMN necrosis and apoptosis by propidium iodide and Annexin V-FITC/PI staining, respectively (Figure 8). Overall, the combination of exogenous ATP or ATP γ S (50 μ M) supplementation and *B. besnoiti* tachyzoite exposure did not change the consistent significant decrease ($p < 0.01$) in anchored and cell-free NET formation driven by NF449 pre-treatments

(Figures 8A, B). As revealed by propidium iodide and Annexin V-based assays, NF449 treatments (10 μ M and 100 μ M) had no effect on PMN necrosis or apoptosis since the proportions of vital PMN remained equal (88.4% and 86.1%, respectively) compared to non-treated controls (87.4%) (Figure 8C). Analysis on NF449-related dose dependence revealed an IC_{50} of 1.27 μ M for *B. besnoiti* tachyzoite-induced NET formation (Figure 8D). In summary, NF449-mediated inhibition of *B. besnoiti* tachyzoite-induced NET formation was dose-dependent and occurred without affecting PMN viability (Figure 8).

3.7 *B. besnoiti* tachyzoite exposure induces a P2X1-dependent clustering of bovine PMN

During co-culture experiments, we noticed that the presence of *B. besnoiti* tachyzoites seemed to drive PMN clustering. To follow this impression and to study whether this finding depended on purinergic signaling, we analyzed parasite-mediated PMN cluster formation in the presence and absence of the P2X1 antagonist

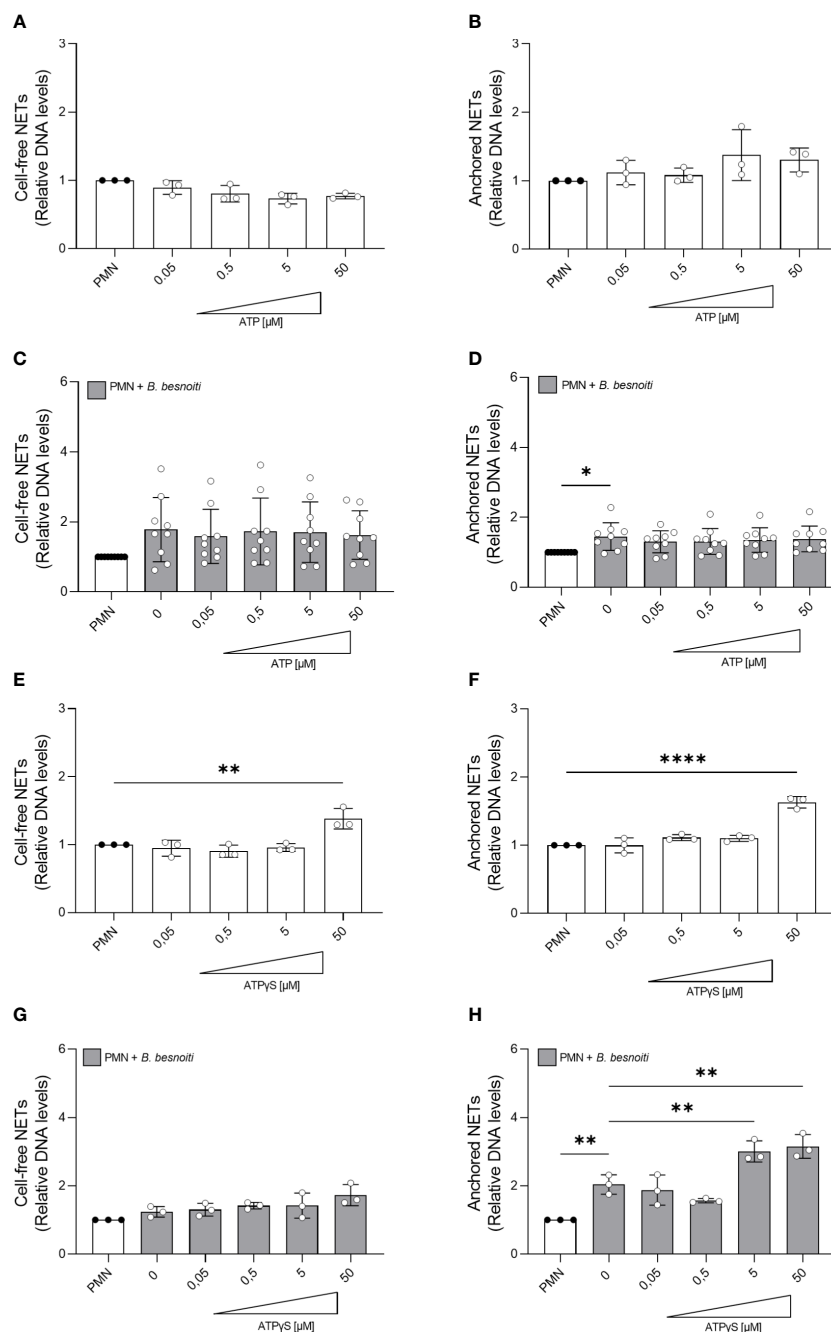


FIGURE 5

ATP γ S supplementation induces NET release and boosts *Besnoitia besnoiti* tachyzoite-driven anchored NET formation. Bovine PMN were pre-treated with increasing concentrations of non-modified ATP or non-hydrolyzable ATP γ S (0.05–50 μM) for 10 min. Then, PMN were incubated for 4 h in plain medium (A, B, E, F) or exposed to *B. besnoiti* tachyzoites (C, D, G, H). After incubation, extracellular DNA was detected and quantified via picogreen-derived fluorescence intensities using a multi-plate reader at 480 nm excitation/520 nm emission wavelengths. All data are shown as mean \pm SD; *p*-values were calculated by one-way ANOVA followed by Dunnett's multiple comparison test. **p* < 0,05; ***p* < 0,01; *****p* < 0,0001.

NF449 (Figure 9). Indeed, an increase ($p < 0.05$) in PMN participating in clusters was verified for *B. besnoiti* tachyzoite-confronted PMN after 4 h of incubation when compared with parasite-free controls (Figure 9B). Notably, the number of PMN participating in clusters decreased to basal levels ($p < 0.01$) when PMN were pre-treated with the P2X1 inhibitor NF449 at a concentration of 100 μM (Figure 9B), thereby confirming the critical role of purinergic signaling in the clustering process.

4 Discussion

In the present study, we studied the role of ATP and purinergic receptor signaling in *B. besnoiti* tachyzoite-induced bovine PMN activation with respect to *i*) PMN energetic state, *ii*) NETosis, and *iii*) PMN clustering. Since the discovery of NETs, there is accumulating evidence that NET formation represents a conserved mechanism among multiple kingdoms (45–47).

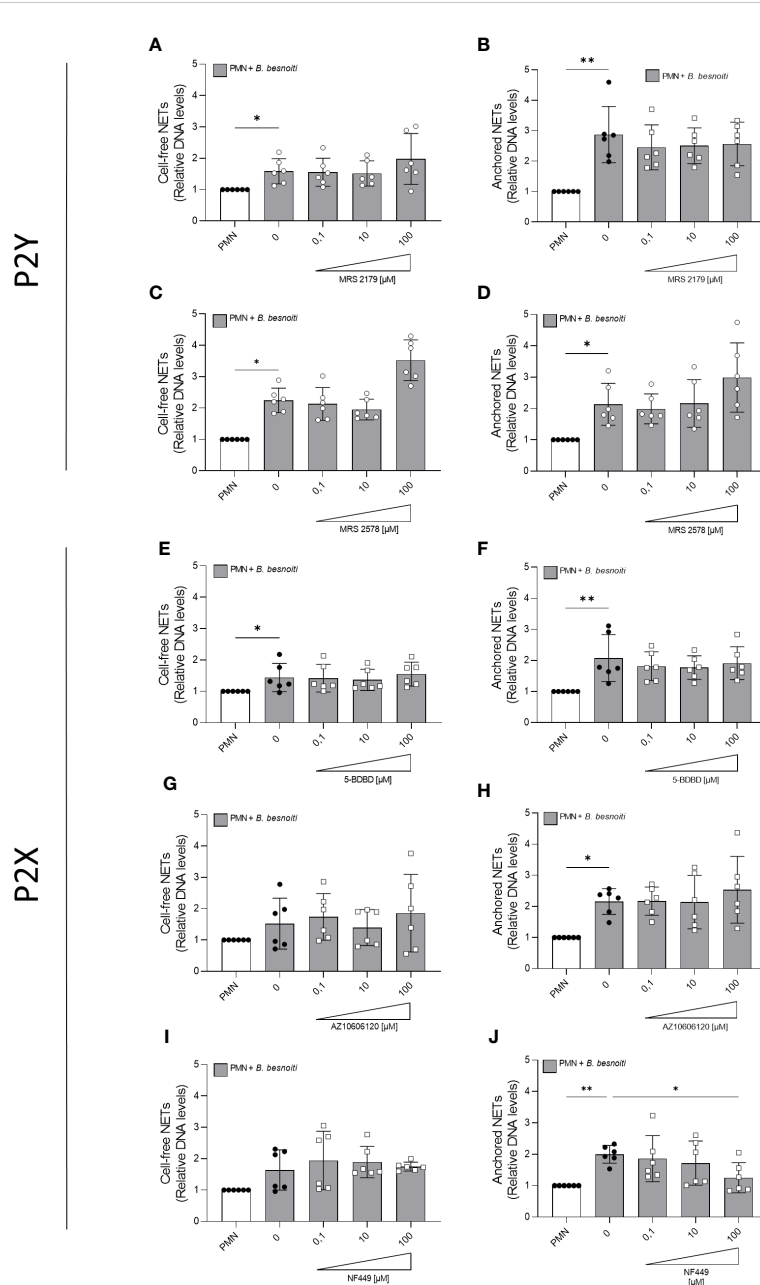


FIGURE 6

Effects of purinergic receptor antagonist pre-exposure treatments on *Besnoitia besnoiti* triggered NET formation. Bovine PMN were pre-treated for 10 min with increasing concentrations of MRS2179, MRS2578, NF449, 5-BDBD, and AZ10606120 (0.1–100 μ M) targeting P2Y1, P2Y6, P2X1, P2X4, and P2X7 receptors, respectively, and then exposed to *B. besnoiti* tachyzoites for 4 (h) Thereafter, cell-free (A, C, E, G, I) and anchored (B, D, F, H, J) NETs were analyzed. For both NET types, extracellular DNA was detected and quantified via picogreen-derived fluorescence intensities using a multi-plate reader at 480 nm excitation/520 nm emission wavelengths. All data are shown as mean \pm SD; *p*-values were calculated by Kruskal-Wallis test followed by Dunn's multiple comparison test (*n* = 6). **p* < 0,05; ***p* < 0,01.

Referring to protozoan parasites, NETosis is efficiently induced by both extra- and intracellular parasites, such as *T. b. brucei*, *T. gondii*, *E. bovis*, *C. parvum*, *N. caninum*, and *B. besnoiti* (21, 24, 26–28, 31–33, 43, 48–51). In the current study, we confirmed the PMN release of DNA-rich extracellular structures decorated with H1 and NE in response to vital *B. besnoiti* tachyzoites by SEM and immunofluorescence. The current data are in line with previous reports on NETs triggered by *B. besnoiti* tachyzoites (30–32, 52, 53). Notably also, other innate cell types like primary bovine monocytes

reacted to (M)ETosis when being exposed to *B. besnoiti* tachyzoites (53), thereby emphasizing the general capacity of these parasitic stages to induce this innate effector mechanism and enhancing the likelihood of its occurrence *in vivo* during bovine besnoitiosis.

PMN are considered as highly glycolytic cells and glycolysis is active when PMN are producing ROS or performing phagocytosis (54, 55). Recently, gluconeogenesis and glycogenesis were demonstrated as critical for PMN' lifespan and function, indicating a complex and context-dependent PMN catabolism to

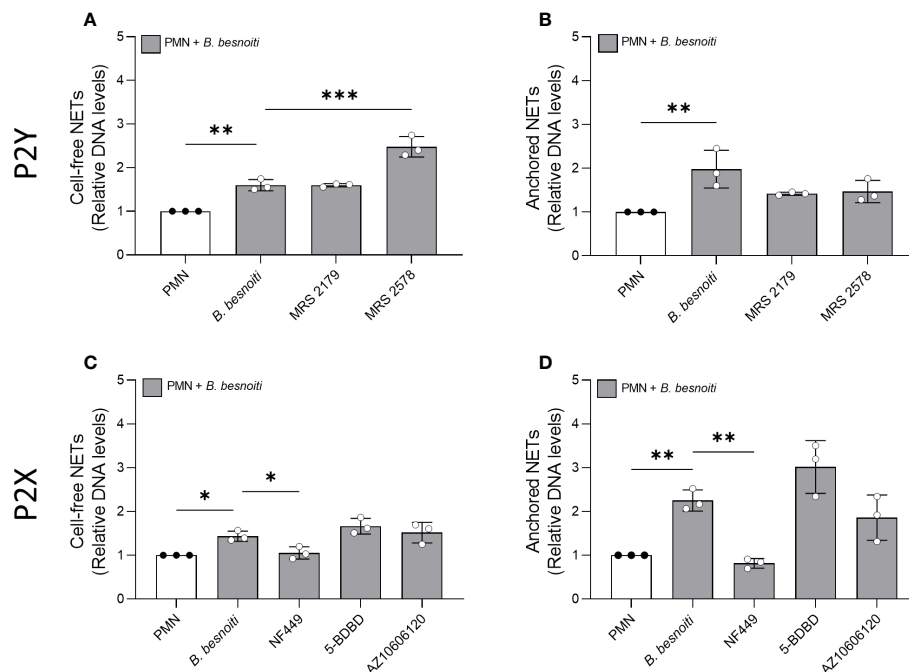


FIGURE 7

Effects of purinergic receptor antagonist post-exposure treatments on *Besnoitia besnoiti* triggered NET formation. Bovine PMN were first exposed to *B. besnoiti* tachyzoites for 40 min and then treated with 100 μ M of MRS2179, MRS2578, NF449, and 5-BDBD targeting P2Y1, P2Y6, P2X1, P2X4, and P2X7 receptors, respectively. After 4 h of incubation, cell-free (A, C) and anchored (B, D) NETs were analyzed. For both NET types, extracellular DNA was detected and quantified via picogreen-derived fluorescence intensities using a multi-plate reader at 480 nm excitation/520 nm emission wavelengths. All data are shown as mean \pm SD; *p*-values were calculated by an ordinary one-way ANOVA with Dunnett's multiple comparison analysis. (*n* = 3). **p* < 0,05; ***p* < 0,01; ****p* < 0,001.

fulfill killing functions (56). In general, PMN-derived oxidative responses (here: OCR) are mainly derived from NOX-based ROS production, with little or no mitochondrial contribution at all (57, 58). In the present study, the early activation of bovine PMN seemed to be related to ROS production without the involvement of glycolysis. Thus, PMN oxidative activity increased at 5-10 min post-*B. besnoiti* tachyzoite exposure, as detected by a continuous increment of OCR values most likely reflecting PMN oxidative burst. This is in line with previous observations using DCFH-DA to measure *B. besnoiti* tachyzoite-induced ROS in PMN (30). These data, even though measured by different techniques, confirm a consistent role of ROS production, accompanied by oxygen consumption in parasite-induced NETs as driven by *T. gondii* (49), *E. bovis* (42), and trypomastigote stages of *T. b. brucei* (28). Overall, *B. besnoiti* tachyzoite-induced oxygen consumption was not influenced by the addition of exogenous ATP or ATP γ S, thereby denying a priming effect of ATP. Intriguingly, *B. besnoiti* tachyzoite-induced NET formation was recently proven as mitochondrial ATP synthase-dependent since it was significantly dampened by oligomycin treatments (32), indicating a potential later relevance (i.e., after 30 min of confrontation) of the mitochondrial activity or mitochondrial ROS to sustain *B. besnoiti* tachyzoite-induced NET formation. Given that ECAR enhancement mirrors the extracellular accumulation of lactate (58), the current data may indicate that immediate bovine PMN reactions to parasite stages may not rely on glycolytic responses. On the other hand, ATP/ATP γ S supplementation led to an acute

(within a few minutes) increase in PMN ECAR. However, when referring to later effector phases by analyzing NET formation after 6 h of co-culture, metabolic signatures of *B. besnoiti* heat-inactivated tachyzoite-exposed bovine PMN showed a significant increase in glucose and serine consumption and glutamate release in addition to a decrease in glutamine release during NETosis, thereby suggesting a switch in parasite-driven metabolic responses toward glycolysis (32). The differences in the current data may rely on the use of heat-inactivated tachyzoites, the presence of cytochalasin to block phagocytosis - likely altering PMN catabolism - and on the later time point compared with the current data (40 min vs 6h), highlighting again the time- and context-dependent nature of PMN responses upon activation (56). Recent evidence on PMN-specific immunometabolism revealed that this innate "differentiated" cell type can indeed selectively induce different metabolic pathways after activation, depending on the effector mechanism to be performed (e.g., chemotaxis, ROS production, NET formation, or degranulation) (59). Overall, in the case of NET formation, there is a general consensus that glycolysis seems to be the main mechanism of energy generation in PMN. However, referring to *B. besnoiti* tachyzoite-driven NETosis (32), the blockage of glycolysis via FDG treatments did not directly affect NET formation. Nevertheless, a key role of pyruvate- and lactate-mediated metabolic pathways for proper tachyzoite-mediated NETosis was demonstrated since chemical inhibition of lactate release via oxamate and dichloroacetate and blockage of pyruvate dehydrogenase, α -ketoglutarate dehydrogenase, and transketolase

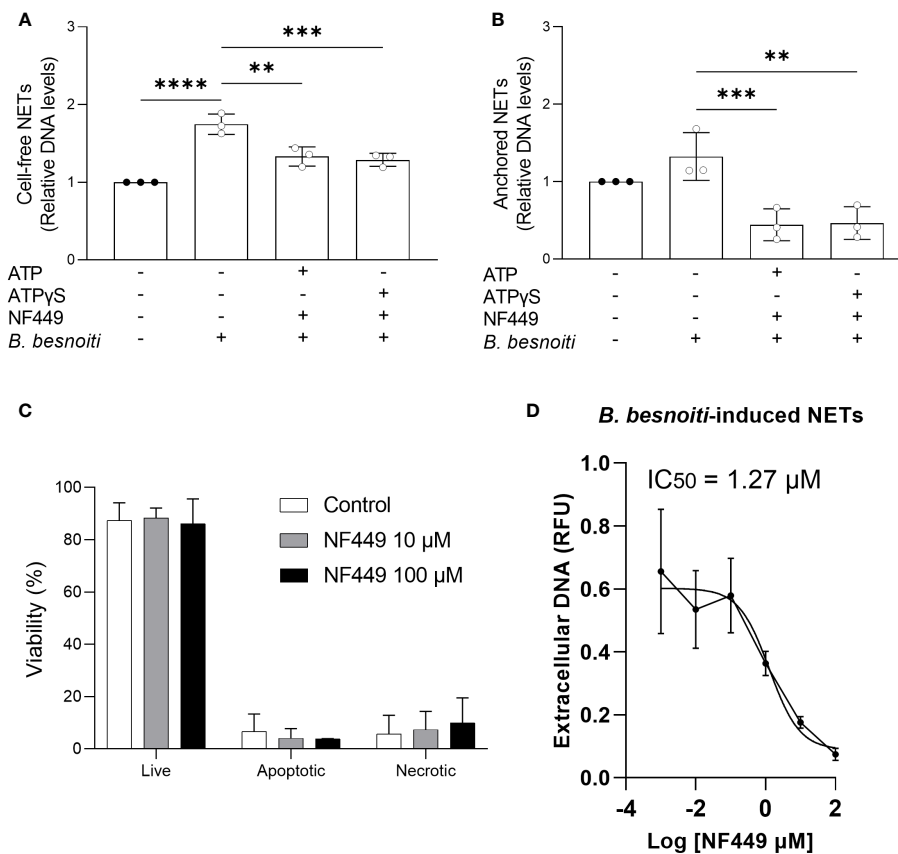


FIGURE 8

NF449 does not affect PMN viability and inhibits *Besnoitia besnoiti* triggered NET formation in an ATP-independent but dose-dependent manner. (A, B) Bovine PMN were pre-treated with NF449 (100 µM) in the presence or absence of ATP/ATPyS and then confronted with *B. besnoiti* tachyzoites. After 4 h of incubation, extracellular DNA was detected and quantified via picogreen-derived fluorescence intensities. (C) Annexin V-FITC and propidium iodide staining of PMN treated with NF449 for 4 h. (D) NF449-based dose-response-inhibition of *B. besnoiti* tachyzoite-induced NET formation. The IC₅₀ was calculated by a nonlinear regression analysis. All data are shown as mean ± SD; *p*-values were calculated by one-way ANOVA with Dunnett's multiple comparison analysis. (*n* = 3). ***p* < 0,01; ****p* < 0,001; *****p* < 0,0001.

via oxythiamine indeed dampened *B. besnoiti* tachyzoite-driven NETosis (32). Comparable NET-related findings were reported for the closely related apicomplexan parasite *E. bovis*. Here, *E. bovis*-triggered NET formation was also not affected by FDG treatments, but by oxamate, oligomycin, and MCT inhibitors (42). Altogether, these data may indicate a pivotal role of secondary metabolites of the carbohydrate catabolism rather than of glycolysis itself in apicomplexan parasite-induced NET formation at times later than 40 min of activation (32, 42).

In general, ATP is either synthesized by mitochondrial respiration or glycolysis. Importantly, ATP not only represents the key energy source of metabolism but also actively participates in the activation of PMN effector function via purinergic signaling. During inflammation or ischemia, several cell types release cellular ATP as a danger and "find me" signal fueling inside-out signaling mechanisms that regulate the activation and function of PMN. Under normal circumstances, the released ATP boosts PMN effector functions like chemotaxis, degranulation, phagocytosis, and NETosis through autocrine feedback mechanisms that involve ATP and adenosine receptors (60, 61). These purinergic signaling mechanisms regulate calcium influx and other

downstream signaling pathways that are required for proper PMN functionality. Overall, a complex network of metabolic pathways regulates ATP release and purinergic signaling mechanisms. This network involves mitochondria that produce the ATP which fuels purinergic signaling. Thus, mitochondria are the link between metabolic and calcium signaling events and the purinergic signaling mechanisms that regulate immune cell functions. Pre-treatments of bovine PMN with oligomycin (blocking mitochondrial ATP synthase) entirely abolished *B. besnoiti* tachyzoite-induced cell-free NET formation, thereby indicating the relevant role of mitochondrial ATP production and purinergic signaling for effective parasite-driven NETosis. In order to study the paracrine effects of ATP, we quantified both extracellular and total ATP concentrations in cultures of *B. besnoiti* tachyzoite-confronted PMN. In supernatants of unstimulated control PMN, an extracellular ATP concentration ([ATP]) of 27.3 nM and 22.6 nM was detected after 15 s and 15 min, respectively. Moreover, a total cellular [ATP] of 334.2 nM (334 fmol/cell) was measured in untreated bovine PMN. In human PMN, the reported ATP intracellular concentration is 1.9 fmol/cell (55). In contrast, under physiological conditions, extracellular

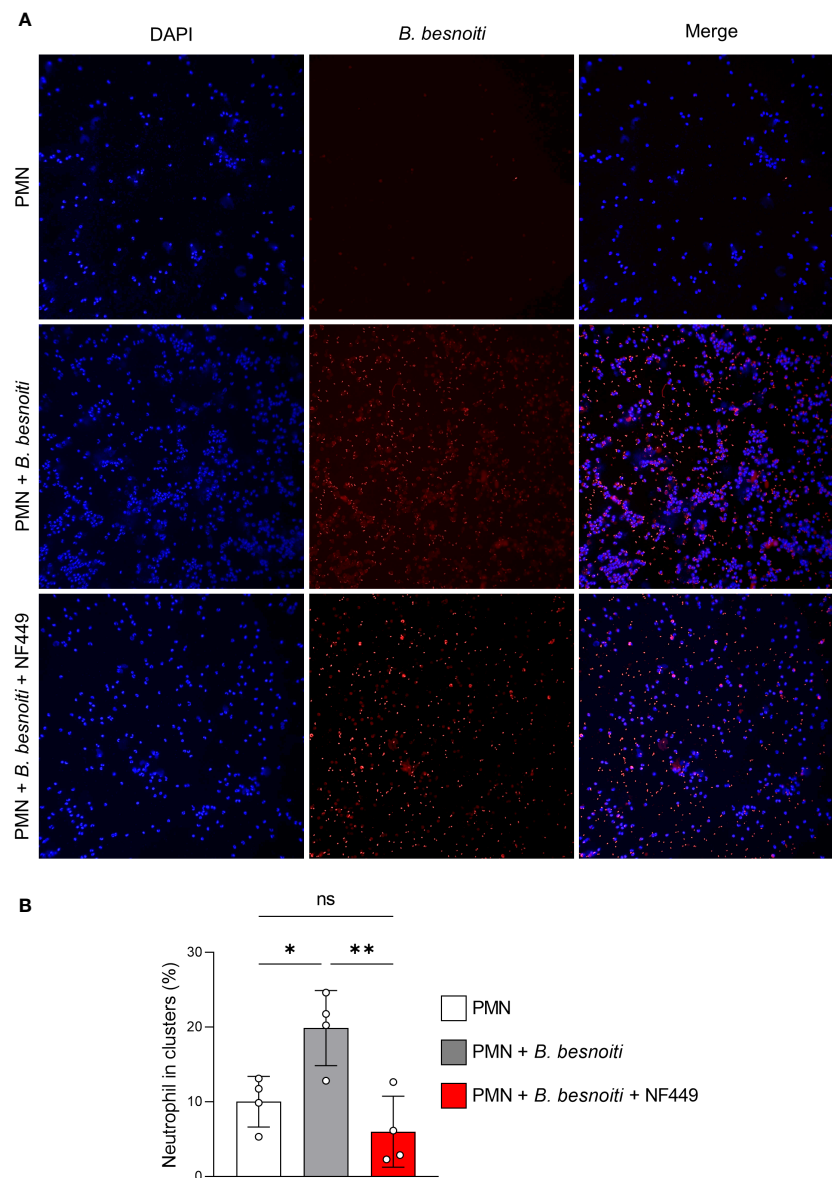


FIGURE 9

B. besnoiti tachyzoite-induced clustering of bovine PMN depends on P2X1-based purinergic signaling. PMN were co-cultured with tachyzoites for 4 h in the presence or absence of NF449 (100 μ M). (A) Exemplary illustrations of tachyzoite-PMN co-cultures stained for DNA (DAPI, blue) and parasite stages (red). (B) DANA-based quantification of cluster formation. All values are presented as mean \pm SD, and *p*-values were calculated using one-way ANOVA followed by Tukey's multiple comparisons. (*n* = 4). **p* < 0,05; ****p* < 0,01.

[ATP] is typically low (< 1 μ M) (62, 63). Whilst current data on extracellular [ATP] match typical basal concentrations, current total cellular [ATP] values seemed rather high; however detailed reference data for bovine PMN are currently missing in the literature. Interestingly, recent data proved that PMN express Cx43 and Panx1 hemi-channels mediating ATP release linked to autocrine purinergic signaling which finally regulates PMN chemotaxis (61). In this context, supplementation of exogenous non-hydrolyzable ATP (ATP γ S), but not of non-modified ATP, significantly induced cell-free and anchored NET formation. Moreover, ATP γ S supplementation enhanced anchored NET formation in *B. besnoiti* tachyzoite-exposed PMN. In general, ATP levels of the extracellular environment are tightly controlled

and eventually lowered by the conversion of different cell types that express plasma membrane ectonucleotidases, such as nucleoside triphosphate diphosphohydrolase 1 (CD39, convert ATP/ADP to AMP) and ecto-5'-nucleotidase (CD73, convert AMP to ADO). Notably, CD39 and CD73 are both expressed in PMN (64). Thus, these ectonucleotidase activities of bovine PMN may explain both the failure of non-modified ATP supplementation to induce NETs and the potential of ATP γ S (which cannot be hydrolyzed by ectonucleotidases) to successfully trigger this effector mechanism.

Recent studies have highlighted the critical role of autocrine purinergic signaling in different PMN-derived effector mechanisms. Two main classes of membrane receptors mediate the effects of extracellular ATP: metabotropic G protein-coupled P2Y receptors

and ionotropic P2X receptors acting as ligand-gated non-selective cation channels. For P2Y receptors, eight subtypes (P2Y1/2/4/6/11/12/13/14) are known, whereas, for P2X, seven subtypes (P2X1–7) have been found (64, 65). Based on data from mRNA, protein, and functional assays, PMN have been reported to express P2X1, P2X7, P2Y2, and P2Y14, as well as all four ADO receptors (61). In this context, Panx1 hemi-channels rapidly release ATP during PMN chemotaxis from pseudopod protrusions, amplifying chemotactic signals through activation of P2Y2-mediated mTOR signaling at the leading edge (66–68). Furthermore, PMN stimulation with LPS-enhanced phagocytosis of *Escherichia coli* in humans, and these effects were abolished when the P2X1 purinergic receptor was blocked (69). Moreover, an antagonist of P2Y6 suppressed monosodium urate crystal-induced PMN oxidative burst (35, 70) and aggregated NET formation (70). In the current study, the effects of different P2X and P2Y receptor antagonists (MRS2179, MRS2578, NF449, 5-BDBD, and AZ10606120) on tachyzoite-driven NET formation were explored. We showed that exclusive pre-treatments of PMN with the P2X1 antagonist NF449 resulted in a significant reduction of parasite-induced anchored NET formation whilst all other antagonists failed to affect NETosis. Similar results were obtained when applying post-exposure treatments. The NF449-related data in principle confirm the recent findings of Zhou et al. (2020) stating the role of P2X1-mediated purinergic signaling in *B. besnoiti* tachyzoite-mediated NETosis. We furthermore proved that NF449 treatments neither induced apoptotic nor necrotic PMN cell death and elucidated dose-dependent effects of NF449 by estimating an IC₅₀ of 1.27 μM. Given that NF449 treatments also inhibited NET formation induced by *T. b. brucei* (28) and *C. parvum* (43) stages, a conserved P2X1-related mechanism in parasite-driven NETosis may be proposed. As an additional and interesting finding, P2X1-mediated signaling also seemed involved in *B. besnoiti* tachyzoite-mediated clustering of bovine PMN. During PMN-tachyzoite-co-cultures, we consistently observed that PMN tend to form clusters which most probably result from chemotactic and migratory actions. However, pre-treatments of PMN with NF449 significantly diminished the number of PMN forming clusters. Therefore the current study adds new data on the role of P2X1-mediated purinergic signaling in parasite-PMN interactions and expands its importance to further PMN-derived effector mechanisms than NETosis. Future studies will focus on its role in other tachyzoite-driven PMN mechanisms.

Data availability statement

The raw data supporting the conclusions of this article will be made available by the authors, without undue reservation.

Ethics statement

The animal study was approved by Ethic Commission for Experimental Animal Studies of the Federal State of Hesse

(Regierungspräsidium Giessen; GI 18/10 Nr. V 2/2022; JLU-No. 0002_V) and are in accordance to European Animal Welfare Legislation: ART13TFEU and currently applicable German Animal Protection Laws. The study was conducted in accordance with the local legislation and institutional requirements.

Author contributions

AT, CH, and IC: conceptualization and supervision. GE: investigation (PMN isolation, *Besnoitia besnoiti*/MDBK cell culture, Seahorse, Flow cytometry, ATP measurement, and extracellular DNA quantification experiments), formal analyses, data visualization, and writing the original draft. IC: formal analyses and data visualization. LR: obtained epifluorescence microscopy images. GE, IC, LR, CH, and AT: reviewed the manuscript. CH and AT: funding acquisition. All authors contributed to the article and approved the submitted version.

Funding

The present work was financed by the “Deutsche Forschungsgemeinschaft” (DFG project: TA291/4-3). GE was funded by DAAD/BECAS Chile, 2021 (57559515). The publication fees were partially funded by the Open Access Publication Fund from JLU Giessen.

Acknowledgments

The authors would like to acknowledge all staff members of the Institute for Parasitology, JLU Giessen, Germany. We further thank all staff members of JLU Giessen’s large animal teaching and research station Oberer Hardthof. The authors would like to acknowledge Anika Seipp, Institute of Anatomy and Cell Biology, JLU Giessen, Germany, for her technical support in SEM analyses.

Conflict of interest

The authors declare that the research was conducted in the absence of any commercial or financial relationships that could be construed as a potential conflict of interest.

Publisher’s note

All claims expressed in this article are solely those of the authors and do not necessarily represent those of their affiliated organizations, or those of the publisher, the editors and the reviewers. Any product that may be evaluated in this article, or claim that may be made by its manufacturer, is not guaranteed or endorsed by the publisher.

References

- Álvarez-García G, Frey CF, Mora LMO, Schares G. A century of bovine besnoitiosis: an unknown disease re-emerging in Europe. *Trends Parasitol* (2013) 29:407–15. doi: 10.1016/j.pt.2013.06.002
- Hornok S, Fedák A, Baska F, Hofmann-Lehmann R, Basso W. Bovine besnoitiosis emerging in Central-Eastern Europe, Hungary. *Parasit Vectors* (2014) 7:20. doi: 10.1186/1756-3305-7-20
- Jacquet P, Liénard E, Franc M. Bovine besnoitiosis: epidemiological and clinical aspects. *Vet Parasitol* (2010) 174:30–6. doi: 10.1016/j.vetpar.2010.08.013
- Basso W, Schares G, Gollnick NS, Rütten M, Deplazes P. Exploring the life cycle of *Besnoitia besnoiti*—Experimental infection of putative definitive and intermediate host species. *Vet Parasitol* (2011) 178:223–34. doi: 10.1016/j.vetpar.2011.01.027
- Langenmayer MC, Gollnick NS, Majzoub-Altweck M, Scharr JC, Schares G, Hermanns W. Naturally acquired bovine besnoitiosis: histological and immunohistochemical findings in acute, subacute, and chronic disease. *Vet Pathol* (2015) 52:476–88. doi: 10.1177/030098514541705
- Burn GL, Foti A, Marsman G, Patel DF, Zychlinsky A. The neutrophil. *Immunity* (2021) 54:1377–91. doi: 10.1016/j.immuni.2021.06.006
- Liew PX, Kubes P. The neutrophil's role during health and disease. *Physiol Rev* (2019) 99:1223–48. doi: 10.1152/physrev.00012.2018
- Kolaczowska E, Kubes P. Neutrophil recruitment and function in health and inflammation. *Nat Rev Immunol* (2013) 13:159–75. doi: 10.1038/nri3399
- Nathan C. Neutrophils and immunity: challenges and opportunities. *Nat Rev Immunol* (2006) 6:173–82. doi: 10.1038/nri1785
- Brinkmann V, Reichard U, Goosmann C, Fauler B, Uhlemann Y, Weiss DS, et al. Neutrophil extracellular traps kill bacteria. *Science* (2004) 303:1532–5. doi: 10.1126/science.1092385
- Brinkmann V, Zychlinsky A. Neutrophil extracellular traps: is immunity the second function of chromatin? *J Cell Biol* (2012) 198:773–83. doi: 10.1083/jcb.201203170
- Fuchs TA, Abed U, Goosmann C, Hurwitz R, Schulze I, Wahn V, et al. Novel cell death program leads to neutrophil extracellular traps. *J Cell Biol* (2007) 176:231–41. doi: 10.1083/jcb.200606027
- Hahn S, Giaglis S, Chowdury CS, Hösli I, Hasler P. Modulation of neutrophil NETosis: interplay between infectious agents and underlying host physiology. *Semin Immunopathol* (2013) 35:439–53. doi: 10.1007/s00281-013-0380-x
- Parker H, Winterbourn CC. Reactive oxidants and myeloperoxidase and their involvement in neutrophil extracellular traps. *Front Immunol* (2013) 3:424. doi: 10.3389/fimmu.2012.00424
- Ravindran M, Khan MA, Palaniyar N. Neutrophil extracellular trap formation: physiology, pathology, and pharmacology. *Biomolecules* (2019) 9:365. doi: 10.3390/biom9080365
- Neubert E, Meyer D, Rocca F, Günay G, Kwaczala-Tessmann A, Grandke J, et al. Chromatin swelling drives neutrophil extracellular trap release. *Nat Commun* (2018) 9:3767. doi: 10.1038/s41467-018-02623-5
- Thiam HR, Wong SL, Qiu R, Kittisopikul M, Vahabikashi A, Goldman AE, et al. NETosis proceeds by cytoskeleton and endomembrane disassembly and PAD4-mediated chromatin decondensation and nuclear envelope rupture. *Proc Natl Acad Sci USA* (2020) 117(13):7326–37. doi: 10.1073/pnas.1909546117
- Behrendt JH, Ruiz A, Zahner H, Taubert A, Hermosilla C. Neutrophil extracellular trap formation as innate immune reactions against the apicomplexan parasite *Eimeria bovis*. *Vet Immunol Immunopathol* (2010) 133:1–8. doi: 10.1016/j.vetimm.2009.06.012
- Muñoz-Caro T, Mena Huertas SJ, Conejeros I, Alarcón P, Hidalgo MA, Burgos RA, et al. *Eimeria bovis*-triggered neutrophil extracellular trap formation is CD11b-, ERK 1/2-, p38 MAP kinase- and SOCE-dependent. *Vet Res* (2015) 46. doi: 10.1186/s13567-015-0155-6
- Silva LMR, Caro TM, Gerstberger R, Vila-Viçosa MJM, Cortes HCE, Hermosilla C, et al. The apicomplexan parasite *Eimeria arloingi* induces caprine neutrophil extracellular traps. *Parasitol Res* (2014) 113:2797–807. doi: 10.1007/s00436-014-3939-0
- Abi Abdallah DS, Lin C, Ball CJ, King MR, Duhamel GE, Denkers EY. *Toxoplasma gondii* triggers release of human and mouse neutrophil extracellular traps. *Infect Immun* (2012) 80:768–77. doi: 10.1128/IAI.05730-11
- Reichel M, Muñoz-Caro T, Sanchez Contreras G, Rubio García A, Magdowski G, Gärtner U, et al. Harbour seal (*Phoca vitulina*) PMN and monocytes release extracellular traps to capture the apicomplexan parasite *Toxoplasma gondii*. *Dev Comp Immunol* (2015) 50:106–15. doi: 10.1016/j.dci.2015.02.002
- Yildiz K, Gokpinar S, Gazayagci AN, Babur C, Sursal N, Azkur AK. Role of NETs in the difference in host susceptibility to *Toxoplasma gondii* between sheep and cattle. *Vet Immunol Immunopathol* (2017) 189:1–10. doi: 10.1016/j.vetimm.2017.05.005
- Muñoz-Caro T, Lendner M, Dausgries A, Hermosilla C, Taubert A. NADPH oxidase, MPO, NE, ERK1/2, p38 MAPK and Ca²⁺ influx are essential for *Cryptosporidium parvum*-induced NET formation. *Dev Comp Immunol* (2015) 52:245–54. doi: 10.1016/j.dci.2015.05.007
- Villagra-Blanco R, Silva LMR, Gärtner U, Wagner H, Failing K, Wehrend A, et al. Molecular analyses on *Neospora caninum*-triggered NETosis in the caprine system. *Dev Comp Immunol* (2017) 72:119–27. doi: 10.1016/j.dci.2017.02.020
- Villagra-Blanco R, Silva LMR, Muñoz-Caro T, Yang Z, Li J, Gärtner U, et al. Bovine polymorphonuclear neutrophils cast neutrophil extracellular traps against the abortive parasite. *Neospora caninum* *Front Immunol* (2017) 8:606. doi: 10.3389/fimmu.2017.00606
- Wei Z, Hermosilla C, Taubert A, He X, Wang X, Gong P, et al. Canine neutrophil extracellular traps release induced by the apicomplexan parasite. *Neospora caninum* *In Vitro Front Immunol* (2016) 7:436. doi: 10.3389/fimmu.2016.00436
- Grob D, Conejeros I, Velásquez ZD, Preußner C, Gärtner U, Alarcón P, et al. *Trypanosoma brucei brucei* Induces Polymorphonuclear Neutrophil Activation and Neutrophil Extracellular Traps Release. *Front Immunol* (2020) 11:559561. doi: 10.3389/fimmu.2020.559561
- Maksimov P, Hermosilla C, Kleinertz S, Hirzmann J, Taubert A. *Besnoitia besnoiti* infections activate primary bovine endothelial cells and promote PMN adhesion and NET formation under physiological flow condition. *Parasitol Res* (2016) 115:1991–2001. doi: 10.1007/s00436-016-4941-5
- Muñoz Caro T, Hermosilla C, Silva LMR, Cortes H, Taubert A. Neutrophil Extracellular Traps as Innate Immune Reaction against the Emerging Apicomplexan Parasite *Besnoitia besnoiti*. *PLoS One* (2014) 9:e91415. doi: 10.1371/journal.pone.0091415
- Zhou E, Conejeros I, Velásquez ZD, Muñoz-Caro T, Gärtner U, Hermosilla C, et al. Simultaneous and positively correlated NET formation and autophagy in *Besnoitia besnoiti* tachyzoite-exposed bovine polymorphonuclear neutrophils. *Front Immunol* (2019) 10:1131. doi: 10.3389/fimmu.2019.01131
- Zhou E, Conejeros I, Gärtner U, Mazurek S, Hermosilla C, Taubert A. Metabolic requirements of *Besnoitia besnoiti* tachyzoite-triggered NETosis. *Parasitol Res* (2020) 119:545–57. doi: 10.1007/s00436-019-06543-z
- Zhou E, Silva LMR, Conejeros I, Velásquez ZD, Hirz M, Gärtner U, et al. *Besnoitia besnoiti* bradyzoite stages induce suicidal- and rapid vital-NETosis. *Parasitology* (2020) 147:401–9. doi: 10.1017/S0031812019001707
- Burnstock G, Knight GE. Cellular distribution and functions of P2 receptor subtypes in different systems. *Int Rev Cytol* (2004), 31–304. doi: 10.1016/S0074-7696(04)40002-3
- Chen Y, Yao Y, Sumi Y, Li A, To UK, Elkhail A, et al. Purinergic signaling: a fundamental mechanism in neutrophil activation. *Sci Signal* (2010) 3:ra45. doi: 10.1126/scisignal.2000549
- Fredholm BB. Adenosine, an endogenous distress signal, modulates tissue damage and repair. *Cell Death Differ* (2007) 14:1315–23. doi: 10.1038/sj.cdd.4402132
- Fredholm BB, Ijzerman AP, Jacobson KA, Klotz KN, Linden J. International Union of Pharmacology. XXV. Nomenclature and classification of adenosine receptors. *Pharmacol Rev* (2001) 53:527–52.
- Di Virgilio F, Ceruti S, Bramanti P, Abbracchio MP. Purinergic signalling in inflammation of the central nervous system. *Trends Neurosci* (2009) 32:79–87. doi: 10.1016/j.tins.2008.11.003
- Fuller SJ, Stokes L, Skarratt KK, Gu BJ, Wiley JS. Genetics of the P2X7 receptor and human disease. *Purinergic Signal* (2009) 5:257–62. doi: 10.1007/s11302-009-9136-4
- Haskó G, Linden J, Cronstein B, Pacher P. Adenosine receptors: therapeutic aspects for inflammatory and immune diseases. *Nat Rev Drug Discov* (2008) 7:759–70. doi: 10.1038/nrd2638
- Qu Y, Ramachandra L, Mohr S, Franchi L, Harding CV, Nunez G, et al. P2X7 receptor-stimulated secretion of MHC class II-containing exosomes requires the ASC/NLRP3 inflammasome but is independent of caspase-1. *J Immunol* (2009) 182:5052–62. doi: 10.4049/jimmunol.0802968
- Conejeros I, López-Osorio S, Zhou E, Velásquez ZD, Del Río MC, Burgos RA, et al. Glycolysis, monocarboxylate transport, and purinergic signaling are key events in *Eimeria bovis*-induced NETosis. *Front Immunol* (2022) 13:842482. doi: 10.3389/fimmu.2022.842482
- Hasheminasab SS, Conejeros I D, Velásquez Z, Borggrefe T, Gärtner U, Kamena F, et al. ATP Purinergic Receptor P2X1-Dependent Suicidal NETosis Induced by *Cryptosporidium parvum* under Physioxia Conditions. *Biology* (2022) 11:442. doi: 10.3390/biology11030442
- Tanaka K, Koike Y, Shimura T, Okigami M, Ide S, Toiyama Y, et al. *In vivo* characterization of neutrophil extracellular traps in various organs of a murine sepsis model. *PLoS One* (2014) 9:e111888. doi: 10.1371/journal.pone.0111888
- Neumann A, Brogden G, von Köckritz-Blickwede M. Extracellular traps: an ancient weapon of multiple kingdoms. *Biology* (2020) 9:34. doi: 10.3390/biology9020034
- Villagra-Blanco R, Silva L, Conejeros I, Taubert A, Hermosilla C. Pinniped- and Cetacean-Derived ETosis Contributes to Combating Emerging Apicomplexan Parasites (*Toxoplasma gondii*, *Neospora caninum*) Circulating in Marine Environments. *Biology* (2019) 8:12. doi: 10.3390/biology8010012
- Worku M, Rehrah D, Ismail HD, Asiamah E, Adjei-Fremah S. A review of the neutrophil extracellular traps (NETs) from cow, sheep and goat models. *Int J Mol Sci* (2021) 22:8046. doi: 10.3390/ijms22158046
- Díaz-Godínez C, Carrero JC. The state of art of neutrophil extracellular traps in protozoan and helminthic infections. *Biosci Rep* (2019) 39:BSR20180916. doi: 10.1042/BSR20180916

49. Miranda FJB, Rocha BC, Pereira MCA, Pereira LMN, de Souza EHM, Marino AP, et al. *Toxoplasma gondii*-induced neutrophil extracellular traps amplify the innate and adaptive response. *mBio* (2021) 12:e01307–21. doi: 10.1128/mBio.01307-21
50. Muñoz-Caro T, Gibson AJ, Conejeros I, Werling D, Taubert A, Hermosilla C. The role of TLR2 and TLR4 in recognition and uptake of the apicomplexan parasite *Eimeria bovis* and their effects on NET formation. *Pathogens* (2021) 10:118. doi: 10.3390/pathogens10020118
51. Omar M, Abdelal H. NETosis in parasitic infections: A puzzle that remains unsolved. *Int J Mol Sci* (2023) 24:8975. doi: 10.3390/ijms24108975
52. Conejeros I, Velásquez ZD, Grob D, Zhou E, Salecker H, Hermosilla C, et al. Histone H2A and Bovine Neutrophil Extracellular Traps Induce Damage of *Besnoitia besnoiti*-Infected Host Endothelial Cells but Fail to Affect Total Parasite Proliferation. *Biology* (2019) 8:78. doi: 10.3390/biology8040078
53. Muñoz-Caro T, Silva LMR, Ritter C, Taubert A, Hermosilla C. *Besnoitia besnoiti* tachyzoites induce monocyte extracellular trap formation. *Parasitol Res* (2014) 113:4189–97. doi: 10.1007/s00436-014-4094-3
54. Fossati G, Moulding DA, Spiller DG, Moots RJ, White MRH, Edwards SW. The mitochondrial network of human neutrophils: role in chemotaxis, phagocytosis, respiratory burst activation, and commitment to apoptosis. *J Immunol* (2003) 170:1964–72. doi: 10.4049/jimmunol.170.4.1964
55. Borregaard N, Herlin T. Energy metabolism of human neutrophils during phagocytosis. *J Clin Invest* (1982) 70:550–7. doi: 10.1172/JCI110647
56. Sadiku P, Willson JA, Ryan EM, Sammut D, Coelho P, Watts ER, et al. Neutrophils fuel effective immune responses through gluconeogenesis and glycogenesis. *Cell Metab* (2021) 33:411–423.e4. doi: 10.1016/j.cmet.2020.11.016
57. Chacko BK, Kramer PA, Ravi S, Johnson MS, Hardy RW, Ballinger SW, et al. Methods for defining distinct bioenergetic profiles in platelets, lymphocytes, monocytes, and neutrophils, and the oxidative burst from human blood. *Lab Invest* (2013) 93:690–700. doi: 10.1038/labinvest.2013.53
58. Pelletier M, Billingham LK, Ramaswamy M, Siegel RM. Extracellular flux analysis to monitor glycolytic rates and mitochondrial oxygen consumption. *Methods Enzymol* (2014), 125–49. doi: 10.1016/B978-0-12-416618-9.00007-8
59. Jeon J-H, Hong C-W, Kim EY, Lee JM. Current understanding on the metabolism of neutrophils. *Immune Netw* (2020) 20:e46. doi: 10.4110/in.2020.20.e46
60. Idzko M, Ferrari D, Eltzschig HK. Nucleotide signalling during inflammation. *Nature* (2014) 509:310–7. doi: 10.1038/nature13085
61. Wang X, Chen D. Purinergic regulation of neutrophil function. *Front Immunol* (2018) 9:399. doi: 10.3389/fimmu.2018.00399
62. Chen Y, Corriden R, Inoue Y, Yip L, Hashiguchi N, Zinkernagel A, et al. ATP release guides neutrophil chemotaxis via P2Y2 and A3 receptors. *Science* (2006) 314:1792–5. doi: 10.1126/science.1132559
63. Trautmann A. Extracellular ATP in the immune system: more than just a “Danger signal” *Sci Signal* (2009) 2:pe6–6. doi: 10.1126/scisignal.256pe6
64. Junger WG. Immune cell regulation by autocrine purinergic signalling. *Nat Rev Immunol* (2011) 11:201–12. doi: 10.1038/nri2938
65. Junger WG. Purinergic regulation of neutrophil chemotaxis. *Cell Mol Life Sci* (2008) 65:2528–40. doi: 10.1007/s00018-008-8095-1
66. Bao Y, Ledderose C, Seier T, Graf AF, Brix B, Chong E, et al. Mitochondria regulate neutrophil activation by generating ATP for autocrine purinergic signaling. *J Biol Chem* (2014) 289:26794–803. doi: 10.1074/jbc.M114.572495
67. Bao Y, Ledderose C, Graf AF, Brix B, Birsak T, Lee A, et al. mTOR and differential activation of mitochondria orchestrate neutrophil chemotaxis. *J Cell Biol* (2015) 210:1153–64. doi: 10.1083/jcb.201503066
68. Weninger W, Biro M, Jain R. Leukocyte migration in the interstitial space of non-lymphoid organs. *Nat Rev Immunol* (2014) 14:232–46. doi: 10.1038/nri3641
69. Wang X, Qin W, Xu X, Xiong Y, Zhang Y, Zhang H, et al. Endotoxin-induced autocrine ATP signaling inhibits neutrophil chemotaxis through enhancing myosin light chain phosphorylation. *Proc Natl Acad Sci* (2017) 114:4483–8. doi: 10.1073/pnas.1616752114
70. Sil P, Hayes CP, Reaves BJ, Breen P, Quinn S, Sokolove J, et al. P2Y6 receptor antagonist MRS2578 inhibits neutrophil activation and aggregated neutrophil extracellular trap formation induced by gout-associated monosodium urate crystals. *J Immunol* (2017) 198:428–42. doi: 10.4049/jimmunol.1600766